Tetraether bolaform amphiphiles as models of archaebacterial membrane lipids: synthesis, differential scanning calorimetry, and monolayer studies

ARTICLE *in* LANGMUIR · FEBRUARY 1992

Impact Factor: 4.46 · DOI: 10.1021/la00038a056

2 AUTHORS, INCLUDING:

David H Thompson
Purdue University
114 PUBLICATIONS **3,179** CITATIONS

SEE PROFILE

Tetraether Bolaform Amphiphiles as Models of Archaebacterial Membrane Lipids: Synthesis, Differential Scanning Calorimetry, and Monolayer Studies

Jong-Mok Kim and David H. Thompson*

Biomolecular Materials Research Group, Department of Chemical and Biological Sciences, Oregon Graduate Institute of Science and Technology, 19600 N.W. von Neumann Drive, Beaverton, Oregon 97006-1999

Received September 26, 1991

Four racemic tetraether lipids containing a single 1,ω-polymethylene chain (ω = 16, 20) bridging two glycerophosphate headgroups (bolaform amphiphiles) have been synthesized. These materials have been characterized at the air-water interface by monolayer balance methods and in buffered solution by differential scanning calorimetry (DSC) and negative stain transmission electron microscopy (TEM). Molecular areas in excess of 100 Å²/molecule at 40 mN/m² were observed for all bolaamphiphiles studied, suggesting a U-shaped molecular conformation that places both phosphate headgroups in the water subphase. Aqueous dispersions of these lipids have thermal and morphological properties that depend on molecular structure and solution pH. Phase transition temperatures (T_c) of the structural isomers, 2,2′-di-*O*-decyl-1,1′-*O*-eicosamethylene-*rac*-diglycero-3,3′-diphosphate (PS20) and 1,1′-di-*O*-decyl-2,2′-*O*-eicosamethylene-3,3′-diphosphate (SS20), were 49 and 38 °C, respectively, at pH 2.5. A reduction in the observed T_c of ~14 °C occurred when the pH was raised to 8.1. The closely related structural analogue, 1,1′-*O*-eicosamethylene-2-*O*-eicosyl-*rac*-diglycero-3,2′,3′-diphosphate (PA20), has a T_c of 85 °C. No phase transition was observed above 5 °C for 2,2′-O-dioctyl-1,1′-O-hexadecylmethylene-*rac*-diglycero-3,3′-diphosphoric acid (PS16). Multilamellar structures with hydrocarbon-region spacings of 24-30 Å and overall lengths approaching 0.3 μm were observed by negative stain electron microscopy. The observed lamellae distance is in good agreement with the membrane thickness expected for a bolaamphiphile in its all-anti conformation.

Introduction

Self-assembling lipid membranes have frequently been proposed as key functional elements in a wide variety of chemical, electronic, and optical devices.[1-8] This is due to their ease of formation, their structural diversity, and their ability to serve as coatings or diffusion barriers. The structure and properties of these materials greatly affect their performance in systems where reactions occurring across the lipid membrane are highly distance-dependent, for example, in transmembrane electron-transfer[9-14] or diffusional processes.[15-18] Thinner membranes are highly desirable for artificial photosynthetic systems to increase the rate of charge transfer across the film. This requirement places greater demands on the thermal and mechanical stability of the membrane materials used to isolate reactants in two different aqueous phases.

Previous attempts at increasing membrane stability have typically focused on polymerization. However, this tactic often creates problems of microheterogeneity, pore formation, and postmodification of the film after cross-linking has occurred.[19-25] We have been investigating a different approach to membrane stabilization based on synthetic bolaamphiphile lipids[3,13,26-35] that are structurally anal-

(1) Lehn, J.-M. *Angew. Chem., Int. Ed. Engl.* **1988**, *27*, 89-112.
(2) Ringsdorf, H.; Schlarb, B.; Venzmer, J. *Angew. Chem., Int. Ed. Engl.* **1988**, *27*, 113-158.
(3) Führhop, J.-H.; Krull, M.; Schulz, A.; Möbius, D. *Langmuir* **1990**, *6*, 497-505.
(4) Rubinstein, I.; Steinberg, S.; Tor, Y.; Shanzer, A.; Sagiv, J. *Nature* **1988**, *332*, 426-429.
(5) Hickman, J. J.; Ofer, D.; Zou, C.; Wrighton, M. S.; Laibinis, P. E.; Whitesides, G. J. *J. Am. Chem. Soc.* **1991**, *113*, 1128-1132.
(6) Bourdillon, C.; Majda, M. *J. Am. Chem. Soc.* **1990**, *112*, 1795-1799.
(7) Bohn, P. W. *Spectroscopy* **1988**, *3*, 38-46.
(8) Tachibana, H.; Nakamura, T.; Matsumoto, M.; Tanaka, M.; Komizu, H.; Manda, E.; Niino, H.; Yabe, A.; Kawabata, Y. In *Molecular Electronics—Science and Technology*; Aviram, A., Ed.; Engineering Foundation: New York, 1989; pp 49-54.
(9) Hurst, J. K.; Thompson, D. H. *J. Membr. Sci.* **1986**, *28*, 3-29.
(10) Nango, M.; Mizusawa, A.; Miyake, T.; Yoshinaga, J. *J. Am. Chem. Soc.* **1990**, *112*, 1640-1642.
(11) Dannhauser, T. J.; Nango, M.; Oku, N.; Anzai, K.; Loach, P. A. *J. Am. Chem. Soc.* **1986**, *108*, 5865-5871.
(12) Tsuchida, E.; Kaneko, M.; Nishide, H.; Hoshino, M. *J. Phys. Chem.* **1986**, *90*, 2283-2284.
(13) Führhop, J.-H.; Fritsch, D.; Tesche, B.; Schmiady, H. *J. Am. Chem. Soc.* **1984**, *106*, 1998-2001.
(14) Takeyama, N.; Sakaguchi, H.; Hashiguchi, Y.; Shimomura, M.; Nakamura, H.; Kunitake, T.; Matsuo, T. *Chem. Lett.* **1985**, 1735-1738.
(15) Patterson, B. C.; Thompson, D. H.; Hurst, J. K. *J. Am. Chem. Soc.* **1988**, *110*, 3656-3657.
(16) Patterson, B. C.; Hurst, J. K. *J. Chem. Soc., Chem. Commun.* **1990**, 1137-1138.
(17) Tabushi, I. *Pure Appl. Chem.* **1982**, *54*, 1733-1736.
(18) Nakagaki, M.; Takagi, R. In *Membranes and Membrane Processes*; Drioli, E., Nakagaki, M., Eds.; Plenum Press: New York, 1986; pp 77-84.
(19) Hayward, J. A.; Castelli, F.; Whittam, M. A.; Johnston, D. S.; Chapman, D. In *Progress in Bioorganic Chemistry and Molecular Biology*; Ovchinnikov, Y. A., Ed.; Elsevier: New York, 1985; pp 335-342.
(20) Leaver, J.; Alonso, A.; Durrani, A.; Chapman, D. *Biochim. Biophys. Acta* **1985**, *727*, 327-335.
(21) Fendler, J. H. *Isr. J. Chem.* **1985**, *25*, 3-10.
(22) Freeman, F. J.; Hayward, J. A.; Chapman, D. *Biochim. Biophys. Acta* **1987**, *924*, 341-351.
(23) Gaub, H.; Buschl, R.; Ringsdorf, H.; Sackmann, E. *Chem. Phys. Lipids* **1985**, *37*, 19-43.
(24) Sackmann, E.; Eggl, P.; Fahn, C.; Bader, H.; Ringsdorf, H.; Schollmeier, M. *Ber. Bunsen-Ges. Phys. Chem.* **1985**, *89*, 1198-1208.
(25) Stefely, J.; Markowitz, M. A.; Regen, S. L. *J. Am. Chem. Soc.* **1988**, *110*, 7563-7469.
(26) Führhop, J.-H.; Liman, U.; Koesling, V. *J. Am. Soc.* **1988**, *110*, 6840-6845.
(27) Führhop, J.-H.; Fritsch, D. *Acc. Chem. Res.* **1986**, *19*, 130-137.
(28) Führhop, J.-H.; Tank, H. *Chem. Phys. Lipids* **1987**, *43*, 193-213.
(29) Bader, H.; Ringsdorf, H. *Faraday Discuss. Chem. Soc.* **1986**, *81*, 329-337.
(30) Yamauchi, K.; Moriya, A.; Kinoshita, M. *Biochim. Biophys. Acta* **1989**, *1003*, 151-160.
(31) Yamauchi, K.; Sakamoto, Y.; Moriya, A.; Yamada, K.; Hosokawa, T.; Higuchi, T.; Kinoshita, M. *J. Am. Chem. Soc.* **1990**, *112*, 3188-3191.
(32) Delfino, J. M.; Stankovic, C. J.; Schreiber, S. L.; Richards, F. M. *Tetrahedron Lett.* **1987**, *28*, 2323-2326.
(33) Diziyou, Y. L.; Genevois, A.; Lazrak, T.; Wolff, G.; Nakatani, Y.; Ourisson, G. *Tetrahedron Lett.* **1987**, *28*, 5743-5746.
(34) Carmichael, V. E.; Dutton, P. J.; Fyles, T. M.; James, T. D.; Swan, J. A.; Zojaji, M. *J. Am. Chem. Soc.* **1989**, *111*, 767-769.

0743-7463/92/2408-0637$03.00/0

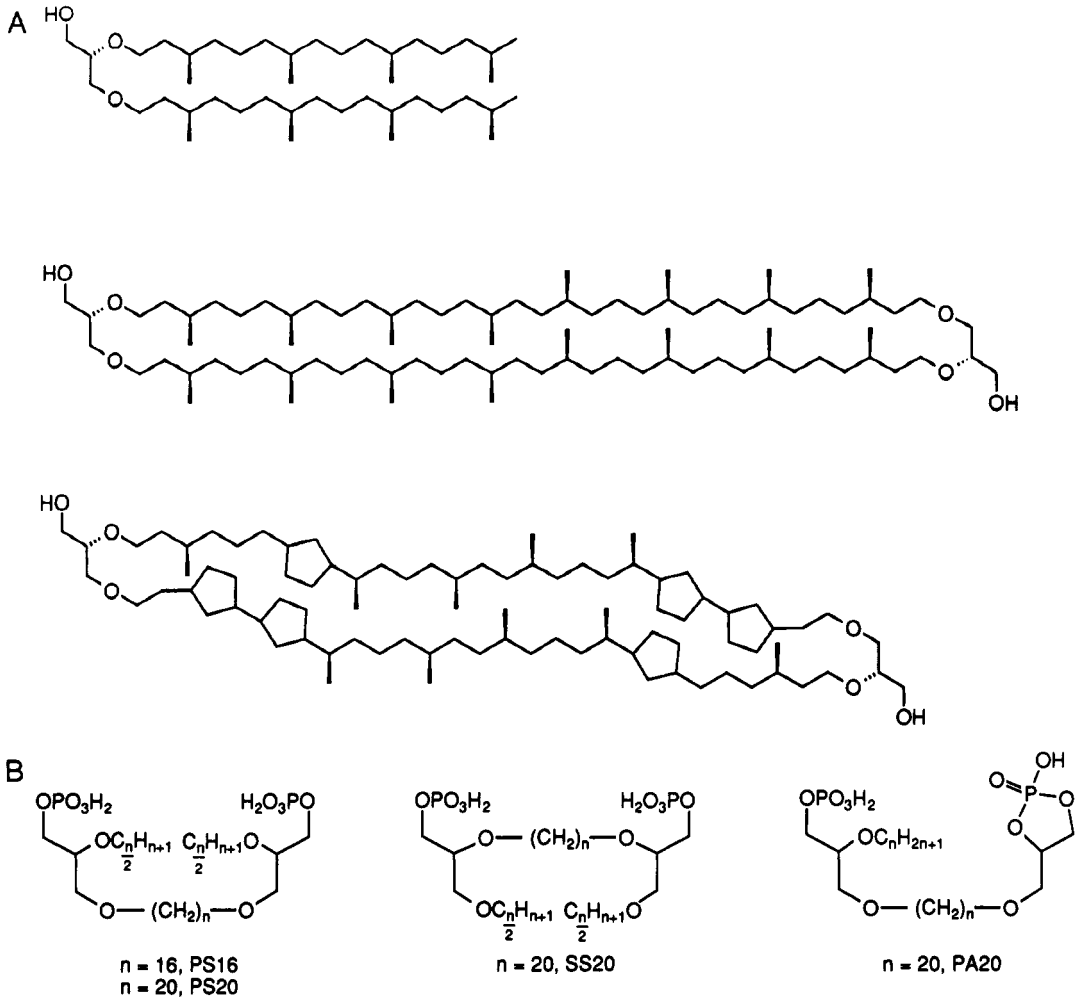

Figure 1. (A) Archaebacterial model membrane lipids. (B) Bolaform model membrane ether lipids.

ogous to those found in thermoacidophilic archaebacteria. The key differences in the membrane lipid structures found in these organisms[36-38] versus those derived from eubacterial sources are ether linkages to glycerol, phytanyl side chains, and biphytanyl "membrane-spanning"[39] hydrophobic segments that often contain cyclopentanoid rings of varying proportions.[40] This paper describes our work with phosphate-containing bolaform amphiphiles (Figure 1) directed toward understanding the relationships between lipid molecular structure, phase behavior, and morphology of their supramolecular assemblies in aqueous solution.

Experimental Methods

Materials. All solvents were reagent grade and distilled before use. Methylene chloride and chloroform were dried and distilled from P_2O_5. Ethyl ether and tetrahydrofuran (THF) were distilled from sodium benzophenone ketyl. Triethylamine and pyridine were distilled from barium oxide. Triphenylmethyl chloride was recrystallized from petroleum ether and acetyl chloride. Phosphorus oxychloride was distilled from sodium metal. Eicosanedioic acid was obtained from American Tokyo Kasei. All other reagents were used as received from Aldrich.

Instruments. Melting points reported are uncorrected. Calorimetric experiments were performed on a Perkin-Elmer DSC-7 using 70-μL sample volumes (0.9 mg/mL) in stainless steel pans. All thermograms were run using the same volume of water or buffer as reference. Monolayer experiments were carried out using a homemade computer-controlled monolayer trough equipped with a Wilhelmy plate. Lipids were spread in the gas expanded state using 80 μL of 0.5 mg/mL solutions in chloroform or THF. After evaporation of the spreading solvent, the film was slowly compressed and the surface pressure measured as a function of molecular area. π–A curves were repeated until three plots were obtained that were reproducible within experimental error. Limiting molecular areas were determined by extrapolating from the slope at the steep rise in surface pressure to the point of zero surface pressure. Samples for microscopy were prepared by sonication (Heat Systems W-225, microtip probe, 5 min at power level 3) of the bolaamphiphile in imidazole-buffered phosphotungstic acid (2%) or ammonium molybdate (2%); a drop of sonicated solution was placed on carbon-coated copper TEM grids, the excess blotted away, and the grid dried in a vacuum desiccator for 1–2 h using an aspirator. The grids were then visualized in a Phillips Model 300 electron microscope at 80 kV. NMR spectra were obtained in $CDCl_3$ using a GE QE-300 or Bruker AMX 400-MHz spectrometer. Fast atom bombardment (FAB) mass spectra were acquired on a VG 7070 EHF spectrometer using polyethylene glycol as matrix and peak matching against 899.54264 and 767.4640.

1,20-Eicosanediol (1). Eicosanedioic acid (15 g, 43.8 mmol) was weighed into a 1-L flask, dissolved in THF with warming, added slowly to a THF solution of $LiAlH_4$ (3 g, 79 mmol) via addition funnel, and heated at reflux for about 20 h. The reaction was then quenched by addition of 5% HCl solution and 200 mL

(35) Lo Nostro, P.; Briganti, G.; Chen, S.-H. *J. Colloid Interface Sci.* **1991**, *142*, 214–223.
(36) Langworthy, T. A. In *The Bacteria, Vol. VIII: Archaebacteria*; Woese, C. R., Wolfe, R. S., Eds.; Academic Press: New York, 1985; pp 459–497.
(37) Luzzati, V.; Gambacorta, A.; DeRosa, M.; Gulik, A. *Annu. Rev. Biophys. Biophys. Chem.* **1987**, *16*, 25–47.
(38) Heathcock, C. H.; Finkelstein, B. L.; Jarvi, E. T.; Radel, P. A.; Hadley, C. R. *J. Org. Chem.* **1988**, *53*, 1922–1942.
(39) While the aliphatic residues of the naturally occurring bolaform lipids are sufficiently long to span the membrane, producing what would be formally a monolayer membrane, transmembrane orientation of these lipids within the biomembrane has not been proven.
(40) DeRosa, M.; Esposito, E.; Gambacorta, A.; Nicolaus, B.; BuLock, J. D. *Phytochemistry* **1980**, *19*, 827–831.

of $CHCl_3$ added. After separation, the organic layer was dried over sodium sulfate and evaporated. The residue was recrystallized from benzene to yield 9.5 g (70% yield) of **1**: mp 95 °C; R_f 0.4 in hexane/ethyl acetate (1:1); ^1H NMR 1.27 (br s, 34 H, $(OH)_2$ and $(CH_2)_{16}$), 1.57 (m, 4 H, $OCCH_2$), 3.64 (t, 4 H, CH_2O).

1,20-Dibromoeicosane (2). 1 (10 g, 31.9 mmol) was weighed into a 250-mL flask with 100 mL of 48% HBr solution. The reaction was stirred at reflux for 24 h and then cooled to room temperature. The aqueous layer was decanted and the remaining dark-brown solid was dissolved in $CHCl_3$ and washed with water until the water phase remained at neutral pH. The organic layer was dried and the product isolated by column chromatography using hexane as eluent: isolated yield, 6.1 g (43%); mp 63 °C; R_f 0.5 in hexane.

A similar procedure was used to prepare 1,16-dibromohexadecane from the commercially available diol in 65% isolated yield: mp 49 °C.

1,1′-*O*-Eicosamethylene-*rac*-disolketal (3). Solketal (14.4 g, 109 mmol) was weighed into a 500-mL flask along with dry THF and NaH (4.4 g, 110 mmol). When gas evolution ceased, **2** (6 g, 13.6 mmol) was added and the mixture heated at reflux until **2** was entirely consumed as determined by TLC (~4 days). The dark-yellow reaction mixture was cooled and filtered through a 1-in. plug of silica gel and the solution concentrated by rotary evaporation. The residue was separated by column chromatography using CH_2Cl_2 to give 4.4 g (60% yield) of **3**: mp 57 °C; R_f 0.7 in CH_2Cl_2; ^1H NMR 1.27 (br s, 32 H, $(CH_2)_{16}$), 1.36 (s, 6 H, acetonide CH_3), 1.41 (s, 6 H, acetonide CH_3), 1.57 (m, 4 H, $OCCH_2$), 3.50 (m, 8 H, OCH_2OCH_2), 3.74 (dd, 2 H, CH_2O), 4.08 (dd, 2 H, CH_2O), 4.29 (m, 2 H, CHO).

1,1′-*O*-Eicosamethylene-*rac*-diglycerol (4a). **3** (4 g, 7.4 mmol) was dissolved in 100 mL of methanol in a 300-mL flask; HCl/H_2O (7 mL/5 mL) was added. The mixture was heated at 60 °C for 2 days and then cooled and concentrated by rotary evaporation. The residue was washed with water and extracted using $THF/CHCl_3$. The organic layer was concentrated to give 2.9 g (85% yield) of **4** recrystallized from ethyl acetate: mp 100 °C; R_f 0.6 in THF; ^1H NMR 1.26 (br s, 32 H, $(CH_2)_{16}$), 1.54 (m, 4 H, $(OCCH_2)_2$), 3.18 (m, 4 H, $(OH)_4$), 3.57–3.65 (m, 10 H, $(OCHCH_2OCH_2)_2$), 3.78 (m, 2 H, OCH_2), 4.12 (m, 2 H, OCH_2).

The homologous 1,1′-*O*-hexadecylmethylene-*rac*-diglycerol (**4b**) was prepared in 80% yield: mp 87 °C.

3,3′-*O*-Bis(triphenylmethyl)-1,1′-*O*-eicosamethylene-*rac*-diglycerol (5). Tetraol **4** (2 g, 4.3 mmol) was dissolved in 150 mL of THF along with pyridine (2.4 g, 30.3 mmol), (dimethylamino)pyridine (0.2 g, 1.64 mmol), and trityl chloride (5.6 g, 20 mmol), and the mixture heated at reflux. A white precipitate formed after 10 min; the color gradually changed to brown-yellow over a 3-day period after which no starting material remained by TLC. The reaction mixture was cooled, insoluble components were filtered, and the mixture was concentrated. The residue was then dissolved in methylene chloride and washed with water, and the organic layer dried with sodium sulfate. The product was isolated by evaportion and separation via Chromatotron using methylene chloride (after removing $R_f = 0$ components by alumina column chromtography): yield, 1.22 g (30%); R_f 0.6 in methylene chloride; ^1H NMR 1.24 (br s, 32 H, $(CH_2)_{16}$), 1.47 (m, 4 H, $(\beta CH_2)_2$), 2.52 (br s, 2 H, $(OH)_2$), 3.15 (m, 4 H, $(\alpha CH_2)_2$), 3.25–3.45 (m, 8 H, $(OCH_2CCH_2O)_2$), 3.84 (m, 2 H, $(OCCHCO)_2$).

2,2′-*O*-Didecyl-3,3′-*O*-bis(triphenylmethyl)-1,1′-*O*-eicosamethylene-*rac*-diglycerol (6). **5** (1 g, 1.05 mmol) was weighed into a suspension of 60% NaH dispersion (0.42 g, 10.5 mmol) in THF. When gas evolution ceased, 1-bromodecane (2.3 g, 10.5 mmol) was added and the mixture heated at reflux for 3 days. After cooling, the soluble components were filtered through a 1-in. alumina column and the solution was concentrated. Isolation by Chromatotron using hexane/CH_2Cl_2 (1:1) gave 0.77 g (60%) of a colorless oil: R_f 0.7 in hexane; ^1H NMR 0.88 (t, 6 H, $(\omega\text{-}CH_3)_2$), 1.25 (br s, 60 H, $(CH_2)_{30}$), 1.50–1.58 (m, 8 H, $(OCCH_2)_4$), 3.17 (m, 4 H, $(Ph_3COCH_2)_2$), 3.38–3.73 (m, 14 H, glycerol CH's and α CH_2's), 7.12–7.47 (m, 30 H, $(C_6H_5)_6$).

2,2′-*O*-Didecyl-1,1′-*O*-eicosamethylene-*rac*-diglycerol (7). Tetraether **6** (0.7 g, 0.57 mmol), methylene chloride (150 mL), and 12% BF_3–methanol complex (1.5 mL) were combined in a 300-mL flask. The mixture immediately turned yellow and was stirred for 1 day at room temperature. The mixture was then washed with water, dried over sodium sulfate, and evaporated. The product was isolated by silica gel column chromatography using hexane/methylene chloride (1:1): isolated yield, 0.34 g (80%); R_f 0.2 in methylene chloride; ^1H NMR 0.88 (t, 6 H, $(\omega\text{-}CH_3)_2$), 1.54–1.59 (m, 8 H, $(OCCH_2)_4$), 3.42–3.76 (m, 20 H, glycerol CH's, α CH_2's, and $(OH)_2$).

2,2′-*O*-Didecyl-1,1′-*O*-eicosamethylene-*rac*-diglycero-3,3′-diphosphoric Acid (8) (PS20). $POCl_3$ (2 g, 13.4 mmol) was dissolved in THF in an argon-purged 250-mL flask. Et_3N (0.3 g, 2.9 mmol) and diol **7** (0.7 g, 0.94 mmol) were dissolved in THF and slowly added to the reaction mixture over a 15-min period at 5 °C. After stirring overnight at room temperature, the solution was filtered, quenched with distilled water (0 °C) and extracted with $CHCl_3$ and water (pH 1–2). The organic layer was dried with sodium sulfate and concentrated by rotary evaporation. The residue was recrystallized from hexane/ethyl acetate (1:1) to give 0.72 g (85% yield) of **8**: mp 44 °C; R_f 0 in $CHCl_3$, THF, and ethyl acetate; ^1H NMR 0.88 (t, 6 H, $(\omega\text{-}CH_3)_2$), 1.3 (s, 60 H, $(CH_2)_{30}$), 1.56 (m, 8 H, $(OCCH_2)_4$), 3.4–3.7 (m, 14 H, $OCCHOCH_2OC$ and α CH_2's), 4.17 (m, 4 H, $(POCH_2)_2$); FAB MS $(M + H^+) = 903.6452$.

1,1′-*O*-Eicosamethylene-2′-*O*-eicosyl-2,3,3′-*O*-tris(triphenylmethyl)-*rac*-diglycerol (9). Tritrityl monoalcohol side product (1 g, 0.84 mmol) from the preparation of intermediate **5** was added to a 60% NaH dispersion (0.1 g, 2.53 mmol) in THF solution. After bubbling ceased, 1-bromoeicosane (0.91 g, 2.53 mmol) was added and the mixture heated at reflux for 3 days. After cooling, the insoluble components were filtered from the reaction mixture through a 1-in. plug of alumina. The filtrate was concentrated and the product isolated by Chromatotron using hexane/CH_2Cl_2 (1:1): isolated yield, 0.48 g (40%); R_f 0.4 in hexane/CH_2Cl_2 (1:1); ^1H NMR 0.88 (t, 3 H, ω-CH_3), 1.25 (br s, 66 H, $(CH_2)_{33}$), 1.54 (m, 6 H, $(OCCH_2)_3$), 3.16–3.95 (m, 16 H, glycerol CH's and α CH_2's), 7.18–7.47 (m, 45 H, $(C_6H_5)_9$).

1,1′-*O*-Eicosamethylene-2-*O*-eicosyl-*rac*-diglycerol (10). The triether intermediate **9** (0.45 g, 0.31 mmol) was deprotected using 12% BF_3–methanol (1 mL) as described for **7** above, except that the reaction time was 2 days: isolated yield, 0.2 g (27%); R_f 0.05 in methylene chloride.

1,1′-*O*-Eicosamethylene-2-*O*-eicosyl-*rac*-diglycerol-2′,3,3′-diphosphoric Acid (11) (PA20). Phosphorylation of **10** (0.1 g, 0.13 mmol) was performed as for **8** using $POCl_3$ (0.08 g, 0.52 mmol) and Et_3N (0.05 g, 0.5 mmol). The residue was recrystallized from methylene chloride and ethyl acetate: purified yield, 0.05 g (43%); mp 79 °C; R_f 0 in $CHCl_3$, THF, and ethyl acetate.

1-*O*-Decyl-*rac*-solketal (12). NaH (1.96 g, 49 mmol), THF, and solketal (5 g, 37.83 mmol) were combined; when hydrogen evolution ceased, 1-bromodecane (12.5 g, 57 mmol) was added to the mixture and the solution heated at reflux for 2 days. The product was isolated as for **3**: isolated yield, 9 g of colorless oil (87%); R_f 0.9 in $CHCl_3$/THF (10:1).

1-*O*-Decyl-*rac*-glycerol (13). Diol deprotection was carried out as for **4** above using **12** (8 g, 29 mmol) and HCl/H_2O (9 mL/7 mL): isolated yield, 5.5 g (82%); R_f 0.4 in $CHCl_3$/THF (10:1).

1-*O*-Decyl-3-*O*-(triphenylmethyl)-*rac*-glycerol (14). A procedure analogous to that described for **5** using diol **13** (5 g, 21.5 mmol), THF (150 mL), Et_3N (3 g, 30 mmol) and (dimethylamino)pyridine (0.2 g, 1.64 mmol) was used. The product was isolated by Chromatotron using methylene chloride after removal of R_f = 0 components by alumina column chromatography: isolated yield, 4.5 g (44%); R_f 0.6 in methylene chloride; ^1H NMR 0.88 (t, 3 H, ω-CH_3), 1.27 (br s, 14 H, $(CH_2)_7$), 1.55 (m, 2 H, $OCCH_2$), 2.57 (s, 1 H, OH), 3.21 (m, 2 H, Ph_3COCH_2), 3.34–3.61 (m, 4 H, OCH_2OCH_2), 3.96 (m, 1 H, OCCHOCO), 7.22–7.57 (m, 15 H, $(C_6H_5)_3$).

1,1′-*O*-Didecyl-2,2′-*O*-eicosamethylene-3,3′-*O*-bis(triphenylmethyl)-*rac*-diglycerol (15). **14** (4 g, 8.4 mmol) and 60% NaH dispersion (0.5 g, 12.6 mmol) in THF were mixed with 1,-20-dibromoeicosane (0.92 g, 2.1 mmol). After heating for 4 days, the product was isolated as for **6** using hexane/CH_2Cl_2 (1:1): isolated yield, 0.5 g (20%); R_f 0.7 in hexane; ^1H NMR 0.88 (t, 6 H, $(\omega\text{-}CH_3)_2$), 1.27 (br s, 60 H, $(CH_2)_{30}$), 1.56 (m, 8 H, $(OCCH_2)_4$), 3.22–3.68 (m, 18 H, glycerol CH's and α CH_2's), 7.2–7.51 (m, 30 H, $(C_6H_5)_6$).

1,1′-*O*-Didecyl-2,2′-*O*-eicosamethylene-*rac*-diglycerol (16). **15** (0.45 g, 0.366 mmol) was deprotected using 12% BF_3–methanol (1.5 mL) and methylene chloride (150 mL) as for **7**. The product was isolated by silica gel column chromatography using hexane and methylene chloride: isolated yield, 0.19 g (70%);

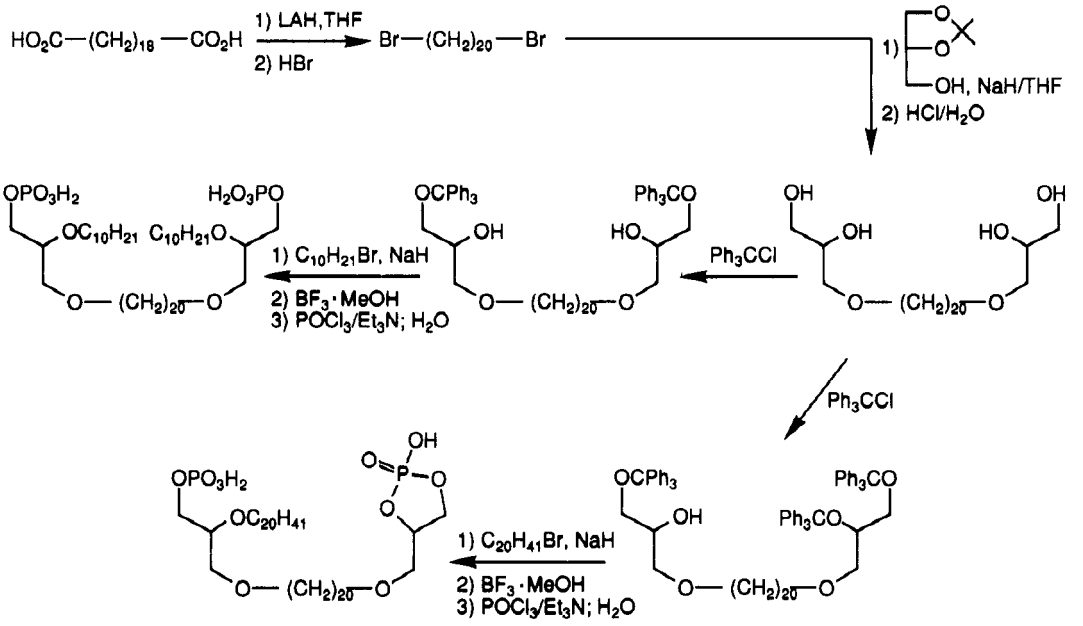

Figure 2. Synthesis of bolaform amphiphiles with 1,1′-polymethylene chains.

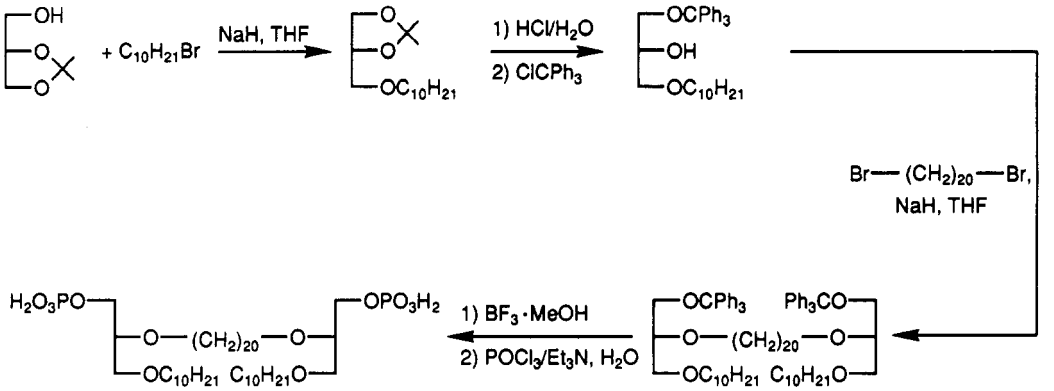

Figure 3. Synthesis of bolaform amphiphiles with 2,2′-polymethylene chains.

R_f 0.2 in methylene chloride; ^{1}H NMR 0.88 (t, 6 H, (ω-CH_3)$_2$), 1.25 (br s, 60 H, $(CH_2)_{30}$), 1.56 (m, 8 H, $(OCCH_2)_4$), 3.42–3.75 (m, 20 H, glycerol CH's, α CH_2's and $(OH)_2$).

1,1′-*O*-Didecyl-2,2′-*O*-eicosamethylene-*rac*-diglycerol-3,3′-diphosphoric Acid (17) (SS20). Phosphorylation using $POCl_3$ (0.6 g, 4.0 mmol), Et_3N (0.08 g, 0.8 mmol), and **16** (0.15 g, 0.2 mmol) was carried out as described for **8** and **11**. The product was recrystallized from hexane/ethyl acetate (1:1) to give 0.095 g (53% purified yield) of **17**: mp 42 °C; R_f 0 in $CHCl_3$, THF, and ethyl acetate; ^{1}H NMR 0.9 (t, 6 H, (ω-CH_3)$_2$), 1.26 (br s, 60 H, $(CH_2)_{30}$), 3.13 (br, 4 H, $(POCH_2)_2$), 3.39–4.22 (m, 14 H, glycerol CH's and α CH2's); FAB MS (M + H$^+$) = 903.6452.

2,2′-*O*-Dioctyl-1,1′-*O*-hexadecylmethylene-*rac*-diglycerol-3,3′-diphosphoric Acid (18) (PS16). The reaction procedure analogous to that for **8** was followed: FAB MS (M + H$^+$) = 791.5187.

Results

A. Synthesis. Ether linkages to glycerol precursors were formed via Williamson synthesis,[41,42] using solketal, 1-bromoalkanes, and 1,ω-dibromoalkanes as starting materials. Synthesis of the isomeric and homologous amphiphiles was accomplished by changing the sequence of diether and monoether bond-forming steps (Figures 2 and 3). Preparations of 1,1′-*O*-hexadecamethylene-*rac*-diglycerol (**4b**) and 1,1′-*O*-eicosamethylene-*rac*-diglycerol (**4a**) were accomplished by heating the corresponding 1,ω-polymethylene dibromide with excess sodium solketalide and subsequent deprotection (Figure 2). The tetraol intermediate was selectively protected with trityl chloride and subjected to a second Williamson step using either octyl or decyl bromide for the C_{16} and C_{20} lipids, respectively. Lewis acid-catalyzed deprotection of these intermediates followed by phosphorylation with $POCl_3$ provided the 1,1′-*O*-hexadecamethylene-2,2′-di-*O*-octyl-rac-diglycero-3,3′-diphosphate (**18**, PS16) and 1,1′-*O*-eicosamethylene-2,2′-di-*O*-decyl-*rac*-diglycero-3,3′-diphosphate (**8**, PS20) in 6–12% overall yield. Extended tritylation of the tetraol followed by alkylation with 1-bromoeicosane, deprotection, and phosphorylation provided 1,1′-*O*-eicosamethylene-2-*O*-eicosyl-*rac*-diglycero-3,2′,3′-diphosphate (**11**, PA20) in 5% yield from 1,1′-*O*-eicosamethylene-*rac*-diglycerol.

A similar approach was used to synthesize 1,1′-di-*O*-decyl-2,2′-*O*-eicosamethylene-3,3′-diphosphate (**17**, SS20) with the exception that the Williamson steps were inverted in the reaction sequence (Figure 3). This pathway afforded SS20 (a structural isomer of PS20) in 2–5% overall yield.

B. Monolayer Experiments. 1. Salt Effect. Monovalent and divalent salts present in the subphase at 1–10 mM concentrations had a small effect on the π–A isotherms of PS20 relative to those obtained on pure water (Figure 4). The apparent limiting molecular area on pure water, ~100 Å^2/molecule, expanded approximately 15% when compressed on 2 mM NaCl subphase. Lower salt concentrations resulted in measured molecular areas that were intermediate between the pure water and 2 mM NaCl

(41) Feuer, H.; Hooz, J. In *The Chemistry of the Ether Linkage*; Patai, S., Ed.; Wiley-Interscience: New York, 1967; pp 445–498.
(42) Bhatia, S. K.; Hajdu, J. *Synthesis* **1989**, 16–20.

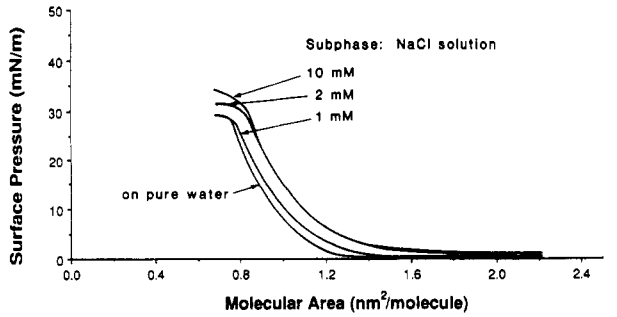

Figure 4. Salt effect on PS20 monolayer films.

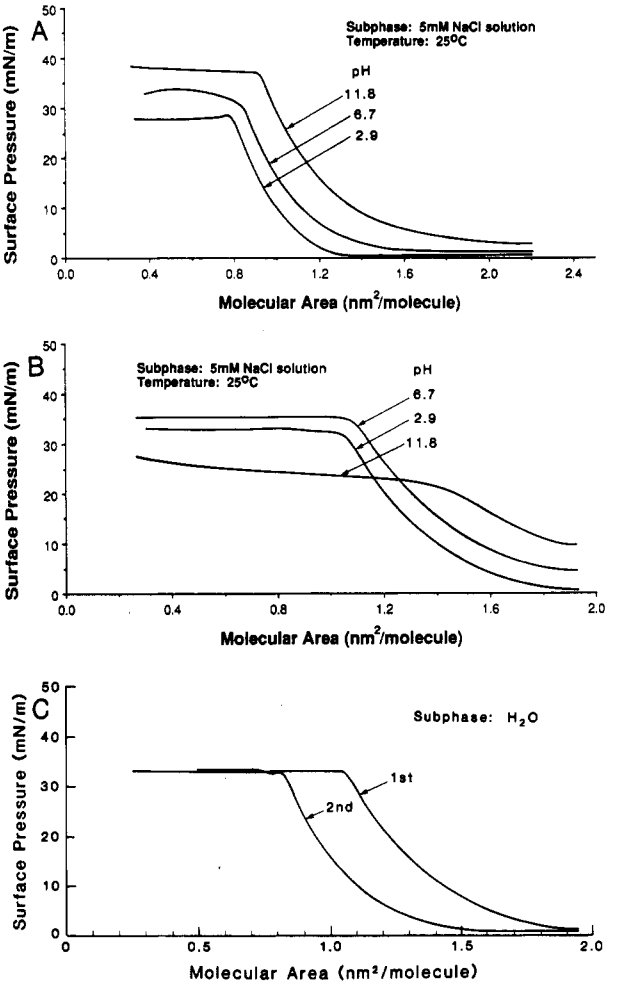

Figure 5. pH and hysteresis effects on bolaform monolayers: A, PS20 isotherms; B, PS16 isotherms; C, PS16 hysteresis.

values. Further increases in NaCl concentration or use of 1 mM $CaCl_2$ in the subphase had little additional effect on the observed molecular area.

2. pH Effect. Larger changes in the π–A curves for PS16 and PS20 were observed as a function of pH (Figure 5A,B). PS20 had a progressively larger molecular area at the air–water interface, from 104 Å^2/molecule to 131 Å^2/molecule, as the subphase pH increased from 2.9 to 11.8 in 5 mM NaCl (Figure 5A). Similar behavior was noted for PS16, except that the areas per molecule were much larger (155 Å^2/molecule versus 115 Å^2/molecule at pH 6.7) and the surface pressure at pH 11.8 was much lower compared to the C_{20} analogue (Figure 5B). Hysteresis of the PS16 film was also observed; reduction in the apparent molecular area from 155 Å^2/molecule to 113 Å^2/molecule occurred upon recompression using pure water as subphase (Figure 5C).

C. Gel Chromatography. Sonication of PS20 in 40 mM imidazole buffer containing 5(6)-carboxyfluorescein (CF) or *N,N'*-dimethyl-4,4'-bipyridinium ion (MV^{2+}) followed by chromatography on Sephadex G-50 gave fractions eluting shortly after the void volume that contained phosphorus[43] but gave no detectable absorbance due to entrapment of either chromophore.

Table I. pH Dependence of PS20 Phase Transitions

pH	T_c, °C	ΔH, J/g	pH	T_c, °C	ΔH, J/g
2.5	50.1	51	7.5	40.3	29.8
3.6	49.6	33.6	8.1	38.8	29.2
4.4	47.8	33.0	9.0	33.3	27.4
6.7	41.6	30.7	10.5	below 10	???

D. Electron Microscopy. PS16, PS20, SS20, and PA20 bolaamphiphiles were sonicated in the presence of imidazole-buffered negative stains (2% ammonium molybdate or 2% phosphotungstic acid), coated onto copper grids, dried, and visualized by transmission electron microscopy. Multilayer structures with alternating light regions (~24–30 Å spacings) and dark regions (~10–12 Å) were observed in the PS16, PS20, and SS20 samples (Figure 6A–C). Lamellae with varying degrees of long-range order were observed in the PS16, PS20, and SS20 cases. Irregular sheetlike structures, also having unstained, light regions measuring ~28 Å thick were observed in micrographs of PA20 (Figure 6D). The addition of 20 mol % cholesterol or DLPC (2:1) did not change the morphology appreciably; however, some curvature of the lamellae was noted (Figure 6E,F).

E. Detergent Dialysis. A 10:1 mixture of detergent (CHAPS, CTAB, cetylpyridinium bromide, or octyl glucoside) and PS20 was vortexed in buffer containing 10 mM MV^{2+} and dialyzed against 500 volumes of buffer as described by Cullis and co-workers.[44] No entrapment of MV^{2+} was observed under these conditions for any of the detergents used. Samples of these dispersions were also studied by electron microscopy (Figure 6G).

F. Differential Scanning Calorimetry. Sonicated dispersions of PS16, PS20, SS20, and PA20 (Figure 7) in pure water were analyzed by DSC between 5 and 90 °C. At pH 2.5, sharp endotherms centered at 50.1 °C were observed for PS20 (ΔH = 51 J/g) in contrast to the two broader endothermic transitions observed for SS20 at 35 and 38 °C. Broad endotherms at ~85 °C were observed for PA20; a smaller broad transition appeared at ~55 °C upon rescanning the sample. Phase transition temperatures of PS20 and SS20 bolas decreased when the pH of the lipid dispersions was raised to 8.1; however, little or no hysteresis was observed in these materials upon rescanning at either pH 2.5 or 8.1. No phase transitions were observed for PS16 in pure water within the temperature range studied.

Discussion

The limiting molecular areas for PS20 (Figure 4) and PS16 after two compression cycles of ~100 Å^2/molecule are similar to those reported by Yamauchi and co-workers for C_{20} and C_{32} bolas;[30] this value is approximately twice that reported for the structurally related ether-linked phosphatidic acid analogues.[45] These monolayer results support a model wherein the bolaform amphiphiles adopt a U-shaped conformation at the air–water interface[30] with no contribution from an elongated, "membrane-spanning" arrangement. Since elongation of the bolas would place

(43) Petitou, M.; Tuy, F.; Rosenfeld, C. *Anal. Biochem.* **1978**, *91*, 350–353.

(44) Wong, K. F.; Parmar, Y. I.; Mayer, L. D.; Pritchard, P. H.; Cullis, P. R. *Biochim. Biophys. Acta* **1987**, *921*, 411–414.

(45) Paltauf, F.; Hauser, H.; Phillips, M. C. *Biochim. Biophys, Acta* **1971**, *249*, 539–547.

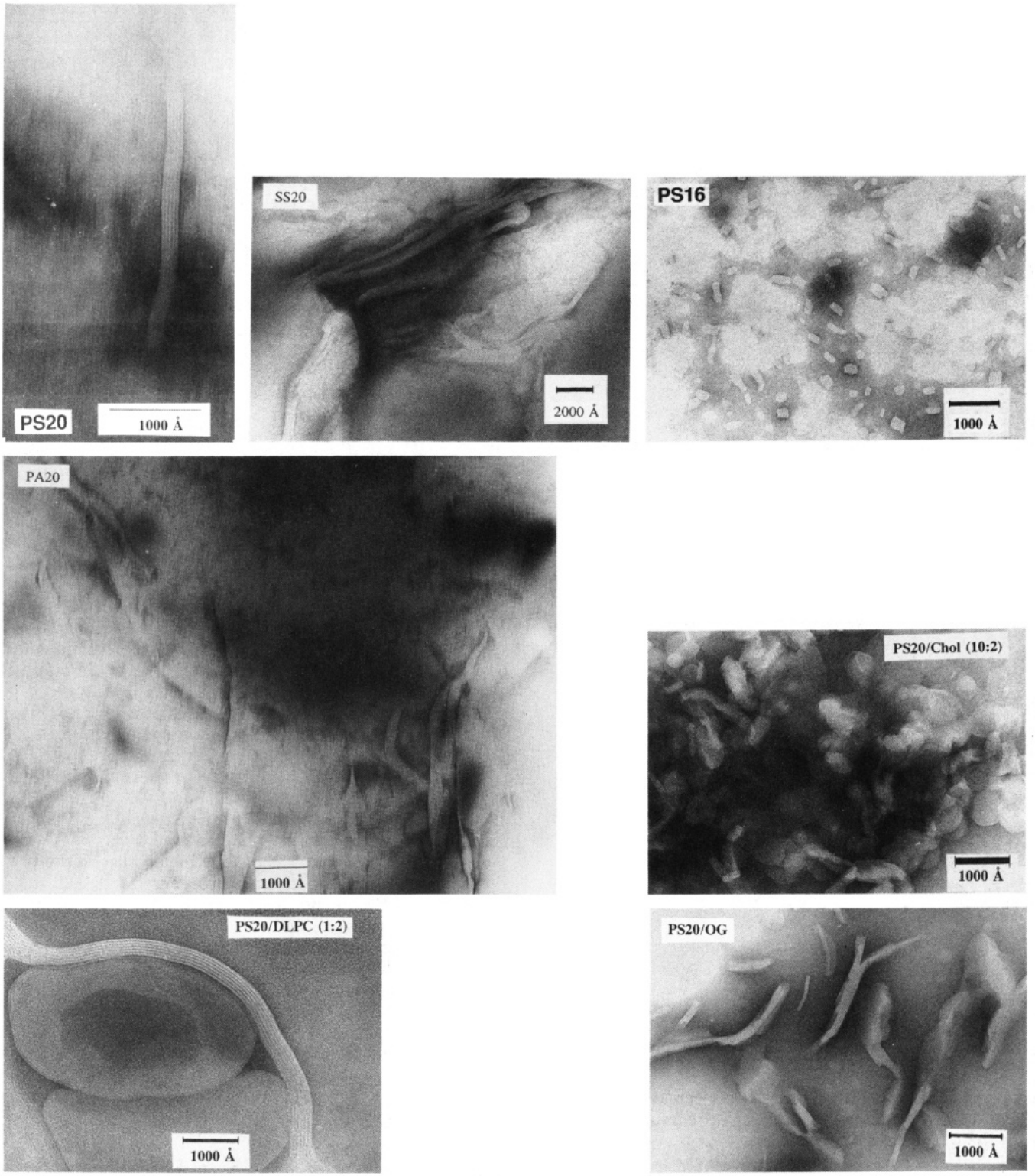

Figure 6. Negative stain transmission electron micrographs: A, PS20; B, SS20; C, PS16; D, PA20; E, PS20 + cholesterol (10:2); F, PS20 + DLPC (1:2); G, PS20 + octyl glucoside.

highly polar phosphate substituents in the nonpolar air phase, curvature of the lipid long molecular axis to accomodate both phosphates in the aqueous subphase occurs instead. This interaction would be energetically favored over the relatively smaller degree of stabilization that would result from increased hydrophobic interactions between lipids in a fully elongated conformation. Similar results have been obtained with monomethyloctadecanedioate[46] and lithocholic acid[47] monolayers (i.e., larger plateau regions at low surface pressures); however, higher surface pressures caused the desorption of the less polar group from the subphase. This is in contrast to the tetraether lipids from *Thermoplasma acidophilum* (having asymmetric glucose and glycerophosphate headgroups); monolayers of these lipids also show a plateau region although the limiting molecular area at its onset occurs at 73 Å^2 per molecule.[48] It is not clear why the natural

(46) Vogel, V.; Möbius, D. *Thin Solid Films* **1985**, *132*, 205–219.

(47) Galvez Ruiz, M. J.; Cabrerizo Vilchez, M. A. *Colloid Polym. Sci.* **1991**, *269*, 77–84.

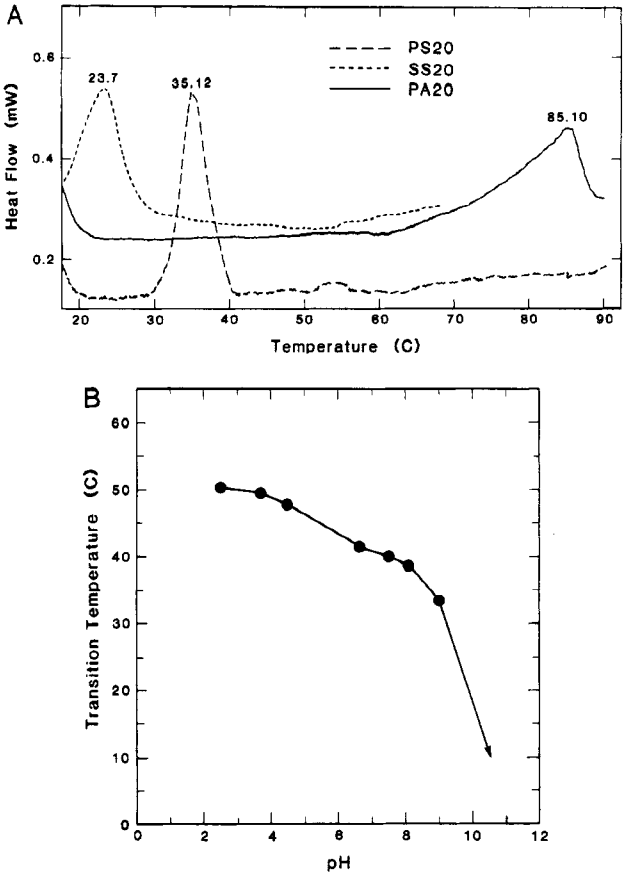

Figure 7. Differential scanning calorimetry of sonicated bolaform amphiphiles: A, PS20, SS20, PA20 at pH 8.1; B, pH effect on T_c.

membrane lipid assumes an elongated configuration at the air–water interface. This may occur as a result of intermolecular hydrogen bonding between the glucose residues, thereby reducing their interactions with the subphase.

Bolaform amphiphile film structuring inferred from these monolayer experiments, however, is not an essential component of the solution model. Since the film balance provides only a two-dimensional aqueous subphase region (unlike the three-dimensional aqueous environment where the dispersed bola can pack into lamellar structures as a transmembrane form), the U-shaped configuration represents the lowest energy conformation possible at the air–water interface, but not necessarily the lowest energy form available within the solution aggregates. Monolayer experiments, therefore, can be misleading for describing bolaamphiphile orientation in water dispersions when two or more highly polar headgroups are present.

The larger molecular areas observed with PS16 and PS20 monolayer films as the pH of the subphase was increased (Figure 5A,B) are consistent with an increase in electrostatic repulsions as the phosphate headgroups are titrated from their fully protonated to their fully deprotonated, tetraanion state.[49] The small changes that occur in PS20 limiting molecular area as NaCl concentrations are increased (Figure 4) imply that the pH-induced changes are due to electrostatic charging effects and not simply attributable to the presence of salt in the subphase. Observed decreases in the onset of liquid-condensed state surface pressure for PS16 as the pH increased to 11.8 is attributed to dissolution of the highly charged bolalipid into the aqueous subphase. This does not occur with PS20, presumably due to the lower water solubility of this material.

Limiting molecular areas measured at room temperature for PS16 were larger than those determined for PS20. We infer from these experiments that PS16 is in a more expanded, fluidlike state than PS20; electrostatic repulsion predominates in the case of PS16 where there are fewer van der Waals interactions to compensate for film expansion due to charge effects. This view is consistent with both the reported effect of pH on phosphatidylglycerol phosphate monolayers[50] and the phase transitions observed for these two lipids determined by calorimetry at pH 8.0 (T_c = 35.7 °C for PS20 and T_c < 5 °C for PS16).

Phase transition temperatures determined for PS20, SS20, and PA20 were found to be both molecular structure- and pH-dependent. In 0.2 M imidazole buffered solution (pH 8.0), the PS20 T_c was 35.7 °C, in contrast to the 7.2 °C transition temperature reported for C_{20} bola with phosphatidylcholine headgroups[31] in pure water. The observed phase transitions for all bolaform amphiphiles studied occurred at higher temperatures as the pH of the solution was lowered. SS20 (Figure 1B) had a lower T_c than the PS20 analogue under all conditions studied, perhaps due to irregular packing at the glycerophosphate interface, while the T_c of PA20 was higher on the first scan. The increased T_c of PA20 may be due to better packing of the eicosamethylene–eicosyl chains relative to the eicosamethylene–decyl chains of PS20 and SS20. We interpret these results as an indication that intermolecular packing and van der Waals interactions in the lamellar state are favored by (1) matching chain lengths and (2) reducing the interfacial electrostatic charge repulsion as the extent of phosphate headgroup protonation[49,51] is increased. A similar effect was noted in the monolayer experiments (see section B.2 and Discussion above).

Negative stain electron micrographs (Figure 6A–F) of bolaform amphiphiles dispersed in imidazole buffer at pH 8.1 show well-developed lamellar morphologies. PS20 forms stacked lamellae having thicknesses of 24–30 Å and lengths of >2000 Å.[52] The structural isomer, SS20, forms more disordered stacked lamellae with different overall dimensions (24–30 Å × 1000–1500 Å). PS16 and PA20 also have lamellar morphologies with smaller-length scales (30+ Å × 200+ Å) occurring with PS16 than for PA20 (30+ Å × >2000 Å). Cosonication of PS20 with either 20 mol % cholesterol or DLPC (2:1) produced slightly curved lamellae, unilamellar vesicles, and multilamellar vesicles. PS20 samples prepared by detergent dialysis with either CHAPS, CTAB, cetylpyridinium bromide, or octyl glucoside all gave stacked lamellae morphologies. Dispersions of PS20 at pH 11 or in the presence of (2:1) tetrabutylammonium hydroxide resulted in small-scale lamellar clusters. These results are consistent with observations made by freeze–fracture electron microscopy.[52]

Conclusions and Speculations

Bolaform amphiphiles synthesized for this study were found to have unusual physical properties in aqueous

(48) Strobl, C.; Six, L.; Heckmann, K.; Henkel, B.; Ring, K. *Z. Naturforsch.* **1985**, *40c*, 219–222.

(49) Van Dijck, P. W. M.; de Kruijff, B.; Verkleij, A. J.; van Deenen, L. L. M.; and de Gier, J. *Biochim. Biophys, Acta* **1978**, *512*, 84–96.

(50) Quinn, P. J.; Kates, M.; Tocanne, J.-F.; Tomoaia-Cotisel, M. *Biochem. J.* **1989**, *261*, 377–381.

(51) Blume, A.; Eibl, H. *Biochim. Biophys. Acta* **1979**, *558*, 13–21.

(52) Similar structures have been reported to arise from staining- and drying-induced artifacts (Talman, Y. *J. Colloid Interface Sci.* **1983**, *93*, 366–382); however, we have confirmed the presence of a lamellar phase by ^{31}P NMR, Raman spectroscopy, and freeze–fracture electron microscopy: Kim, J.-M.; Humphry-Baker, R.; Wong, K. F.; Rananavare, S.; Thompson, D. H. Unpublished results.

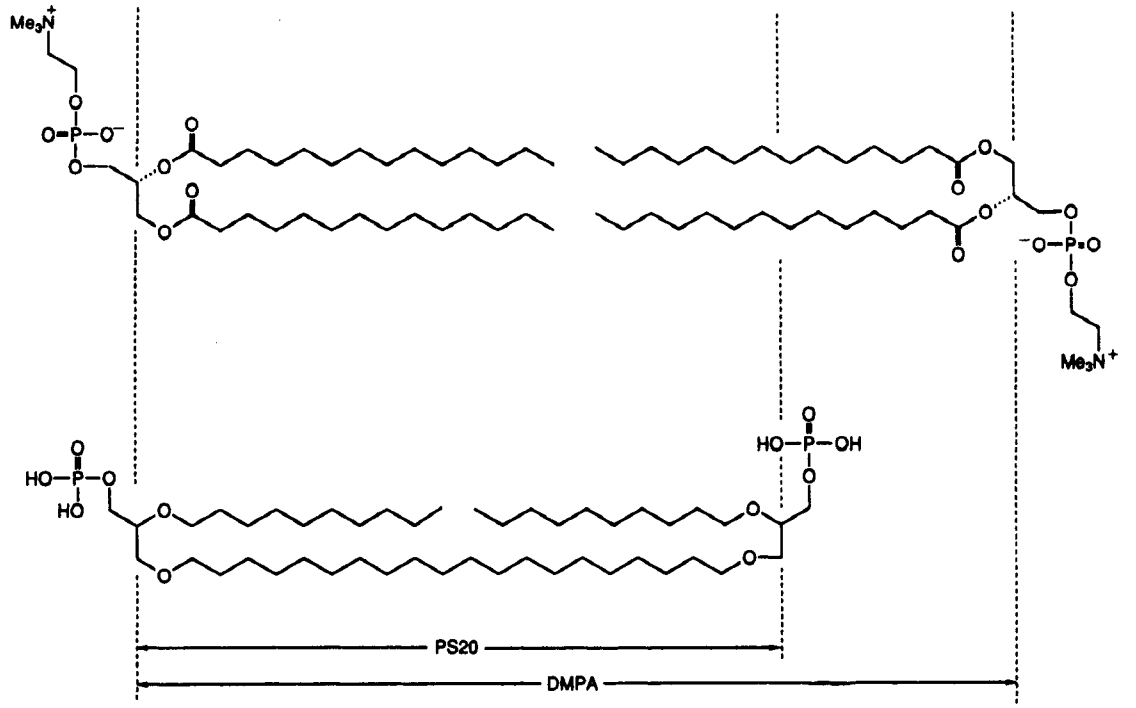

Figure 8. Comparison of DMPA and PS20 membrane thicknesses.

dispersions when compared to those that form conventional phosphogylceride bilayer lipid membranes. The most striking effects were noted in the morphology and phase transition behavior of these materials. The observed T_c values are much greater than one would expect for a membrane structure having approximately half the normal bilayer width (Figure 8); comparison with 1,2-dimyristoyl-*sn*-glycero-3-phosphoric acid (DMPA, T_c = 50 °C, pH 7.4),[49] 1,2-dilauroyl-*sn*-glycero-3-phosphoric acid (DLPA, T_c = 33.5 °C, pH 6),[53] or 1,2-ditetradecyl-*sn*-glycero-3-phosphoric acid (DTPA, T_c = 61.5 °C, pH 7)[54] indicates that the PS20 bolaform lipid aggregates have phase transitions in the same temperature range even though the bilayer forming lipids have nearly twice the lamellar thickness. From a conceptual viewpoint, the PS20 bolalipids may be viewed as the equivalent of a tail-to-tail dimer of 1,2-didecylglycerophosphoric acid at the ω-termini of the two 1-decyl chains. This gives rise to a monolayer-membrane-forming amphiphile having a hydrophobic domain composed of a total of 38 methylene and two methyl groups. Bilayer membranes composed of DTPA have 52 methylenes and four methyls in the hydrophobic region per pair of DTPA molecules contained within opposing monlayer leaflets. Since the phase transitions of both materials are in approximately the same temperature range, the bolaamphiphile molecular structure may represent a more efficient way to increase the thermal stability (T_c) of lamellar phases on a per unit molecular basis. From the evolutionary strandpoint, the biosynthetic efficiency that would be provided by shorter chain "membrane-spanning" lipids is not as important as the fact that the two headgroup configuration has a "self-anchoring" effect within the lamellar plane—that is, lateral diffusion in the membrane should be slower due to strong hydrophilic interactions of the bolaamphiphile at two points instead of one; this requires a cooperative motion of both headgroups in the same direction to effect lateral motion of the lipid within the plane of the membrane. In addition, the well-ordered lamellar morphology of the symmetrical (PS and SS) bolalipid aggregates may be a result of intermolecular hydrogen bonding between phosphate headgroups that would tend to "freeze-in" conformational disorder in the alkyl chains by inhibiting their free rotation. This effect is diminished in the asymmetric (PA) case due to increased hydrophobic interactions (better chain matching) and decreased hydrogen bonding interactions possible with the cyclic phosphodiester headgroup; taken together, these effects tend to favor the formation of lamellar sheets.

These unique physical properties allude to why thermophilic archaebacteria may have produced lipids with the "membrane-spanning" structural motif. Since these organisms require robust membrane structures for their survival, the utilization of two hydrophilic regions separated by a "membrane-spanning" hydrophobic segment may have been adopted as a means of reducing the permeability of their membranes at high temperature by anchoring the lipid molecules at both membrane interfaces thereby lowering their lateral diffusion rate within the lamellar plane. Very long correlation times measured by EPR for molecular diffusion in archaebacterial membrane extracts[55,56] support this notion. We are currently examining the structure and intralamellar dynamics in greater detail as well as utilizing these synthetic materials in vectorial transmembrane reactions and other surface-mediated processes.

Acknowledgment. The authors gratefully acknowledge the U.S. Department of Energy, Division of Energy Biosciences, Office of Basic Energy Sciences (Grant DE-FG06-88ER13963) for financial support and the assistance provided by Professors David W. Grainger and Robert Uphaus with monolayer experiments.

(53) Blume, A. In *Physical Properties of Biological Membranes and Their Functional Implications*; Hidalgo, C., Ed.; Plenum Press: New York, 1988; pp 71–121.
(54) Harlos, K.; Stumpel, J.; Eibl, H. *Biochim. Biophys. Acta* **1979**, *555*, 409–416.
(55) Bruno, S.; Cannistraro, S.; Gliozzi, A.; DeRosa, M.; Gambacorta, A. *Eur. Biophys. J.* **1985**, *13*, 67–76.
(56) Bruno, S.; Gliozzi, A.; Cannistraro, S. *J. Phys. (Paris)* **1986**, *47*, 1555–1563.